AUTHOR QUERY FORM

AIP American Institute of Physics	**Journal: Appl. Phys. Lett.** **Article Number: 015245APL**	**Please provide your responses and any corrections by annotating this PDF and uploading it according to the instructions provided in the proof notification email.**

Dear Author,

Below are the queries associated with your article; please answer all of these queries before sending the proof back to AIP. Please indicate the following:
Figures that are to appear as color online only (i.e., Figs. 1, 2, 3) _____ (this is a free service).
Figures that are to appear as color online and color in print_____ (fees will apply).

Location in article	Query / Remark: click on the Q link to navigate to the appropriate spot in the proof. There, insert your comments as a PDF annotation.
AQ1	Please provide article title for Ref. 36.
AQ2	Please check and confirm the year and journal title in Ref. 18. Also, please check the DOI for the same.
AQ3	Please check and confirm the author name in Ref. 34. Also, please check the DOI for the same.
AQ4	Please check and confirm the author name and year in Ref. 35. Also, please check the DOI for the same.

Thank you for your assistance.

PROOF COPY [L12-11604R] 015245APL

APPLIED PHYSICS LETTERS **101**, 000000 (2012)

Surface effects on the radiation response of nanoporous Au foams

E. G. Fu,[1,a)] M. Caro,[1] L. A. Zepeda-Ruiz,[2] Y. Q. Wang,[1] K. Baldwin,[1] E. Bringa,[3] M. Nastasi,[4] and A. Caro[1]

[1]*Materials Science in Radiation and Dynamics Extremes, Los Alamos National Laboratory, Los Alamos, New Mexico 87545, USA*

[2]*Physical and Life Sciences Directorate, Lawrence Livermore National Laboratory, Livermore, California 94551, USA*

[3]*CONICET and Instituto de Ciencias Basicas, Universidad Nacional de Cuyo, Mendoza 5500, Argentina*

[4]*Nebraska Center for Energy Sciences Research, University of Nebraska-Lincoln, Lincoln, Nebraska 68508, USA*

(Received 23 August 2012; accepted 15 October 2012; published online xx xx xxxx)

We report on an experimental and simulation campaign aimed at exploring the radiation response of nanoporous Au (np-Au) foams. We find different defect accumulation behavior by varying radiation dose-rate in ion-irradiated np-Au foams. Stacking fault tetrahedra are formed when np-Au foams are irradiated at high dose-rate, but they do not seem to be formed in np-Au at low dose-rate irradiation. A model is proposed to explain the dose-rate dependent defect accumulation based on these results. © *2012 American Institute of Physics*. [http://dx.doi.org/10.1063/1.4764528]

Radiation effects in nuclear materials are a limiting factor in the development of advanced fission reactors and fusion/fusion-fission hybrid concepts as well as spacecraft systems. In nuclear reactors, materials are exposed to harsh environments of intense neutron flux and high radiation damage that cause materials degradation and failure.[1] In deep space and long-term missions, exposure to high radiation flux is a critical constraint in space systems design.[2,3]

The search of radiation tolerant materials focuses nowadays on the properties of interfaces as recombination sites for interstitials, vacancies, and transmutations debris. As interfaces naturally provide these recombination sites, materials research has focused on microstructures with high interface content. Interfaces have been shown to act as sinks for radiation-induced defects leading to a reduction in radiation hardening, and an alleviation of He bubble nucleation and growth.[4–6] Two large families of such materials can readily be mentioned, those having a large amount of nanoscale precipitates, such as the nanostructured ferritic alloys (NFA)[7] (or the oxide dispersed strengthened materials (ODS)[8]), with ultrahigh density of Y-Ti-O rich nano-features,[9] and the multilayered nano-composites.[10] We focus here on a third alternative not studied so far, namely, nanoporous materials. Since the key to perfect radiation endurance is perfect recovery, and since surface are perfect sinks for defects, a porous material with a high surface-to-volume ratio has the potential to be extremely radiation tolerant.

In nanoporous materials, high surface area is provided by the open sponge-like 3D-structure of interconnected ligaments. A fundamental understanding of the radiation tolerance of high surface density nanoporous materials is lacking. Several investigations have focused on mechanical testing of nanoporous materials.[11–14] A limited number of computational studies have focused on the mechanical behavior of solids with large porosity,[15,16] porosity evolution in nanoporous metals,[17–19] and deformation mechanisms and stress effects on nanometer-sized Au ligaments.[20,21]

Our recent model[22] defined a window of radiation endurance which depends on the combined effect of two length scales: (1) a characteristic ligament size as compared to the collision cascade size and (2) a diffusion length for defect annihilation relative to dose-rate. Inside this dimensional window, ligaments are sufficiently small that defect migration to the ligament surface happens faster than the time between cascades (ensuring radiation resistance for a given dose-rate), and still large enough not to be destroyed by the cascade induced melting.

In the present work, we report on an experimental/computational campaign aimed at finding the boundaries of the tolerance window, in particular, in the dose-rate dimension. We performed 400 keV Ne^{++} ions irradiation at 6×10^{10} ions/cm^2/s, 3×10^{11} ions/cm^2/s, and 3×10^{12} ions/cm^2/s, corresponding to dose-rates of 7×10^{-5} dpa/s, 3.5×10^{-4} dpa/s, and 3.5×10^{-3} dpa/s (that we call low, intermediate, and high dose rates) for a total of 1 dpa and used molecular dynamics (MD) computer simulations to explore the behavior of np-Au foams.

Ag-Au thin films were co-deposited on single crystal NaCl (001) substrates by electron beam evaporation method at room temperature under high vacuum (base pressure: 5×10^{-8} Torr). The purity of Au and Ag targets was more than 99.9%. The deposition rate for Ag was 0.35 nm/s and for Au was 0.15 nm/s, respectively. The thickness of the film was 160 nm and the atomic ratio of Ag to Au was approximately 7:3, determined by the combinations of Rutherford backscattering spectrometry (RBS) measurement with 4 MeV ^{4}He ions and RBS analysis program package of RUMP.[23]

After cutting into 3 mm × 3 mm pieces, the Au-Ag thin films were detached from the substrates by dipping into de-ionized water to dissolve NaCl, then transferred with filter paper to a Petri dish containing concentrated nitric acid (70% HNO_3) to dissolve Ag through the salt formation of $AgNO_3$. After 1 h, the specimen was retrieved and rinsed in de-ionized water. A 100 mesh transmission electron microscopy (TEM) grid was used to scoop the specimen from water and allow it to dry at room temperature. TEM

[a)]Electronic addresses: fuengang@gmail.com and efu@lanl.gov.

together with energy-dispersive x-ray spectroscopy (EDX) shows that the Au-Ag thin films were dealloyed completely and np-Au foams were formed without Ag left. The thickness of 160 nm of the np-Au foam after the Ag was completely etched away by nitric acid is equivalent to a fully dense Au film of around 50 nm.

Ion irradiations were performed with a 200 kV Danfysik implanter. The TEM grid with the sample was attached to the implanter stage surface by painting colloidal silver paste to the edge of grid and stage surfaces. The increase of sample temperature during room temperature ion irradiation was kept less than 10 °C by flowing compressed nitrogen gas through the Dewar attached to the sample stage. All irradiations were performed under the same conditions except the irradiation dose-rate, which was varied in order to study its effect on the damage accumulation. The irradiation parameters were 400 keV Ne^{++} ions with a fluence of 8.64×10^{14} ions/cm^2, corresponding to a uniform radiation damage of 1 dpa in the entire thickness of sample, as given by the stopping and range of ions in matter (SRIM)[24] that predicts uniform damage down to 50 nm below the surface for bulk Au density target. Since our samples have a thickness of about 150 nm of low density Au, we conclude that the damage is uniform. A FEI Tecnai F30 analytical microscope with an EDX spectrometer and Gatan CCD camera was used to carry out TEM analysis.

To study the irradiation induced microstructure changes, TEM and high resolution TEM (HRTEM) were performed on both as-prepared and ion-irradiated np-Au foams. Fig. 1 shows TEM micrographs of as-prepared np-Au (a) and ion irradiated np-Au at room temperature at different dose-rates ((b)-(d)). Fig. 1(e) shows the change in ligament size for these np-Au foams as obtained by measurements from TEM micrographs. Significant morphological changes are observed in the ion-irradiated np-Au foams; the comparison of the microstructures reveals irradiation-induced coarsening, going from 26 ± 7 nm before irradiation to approximately 35 nm after

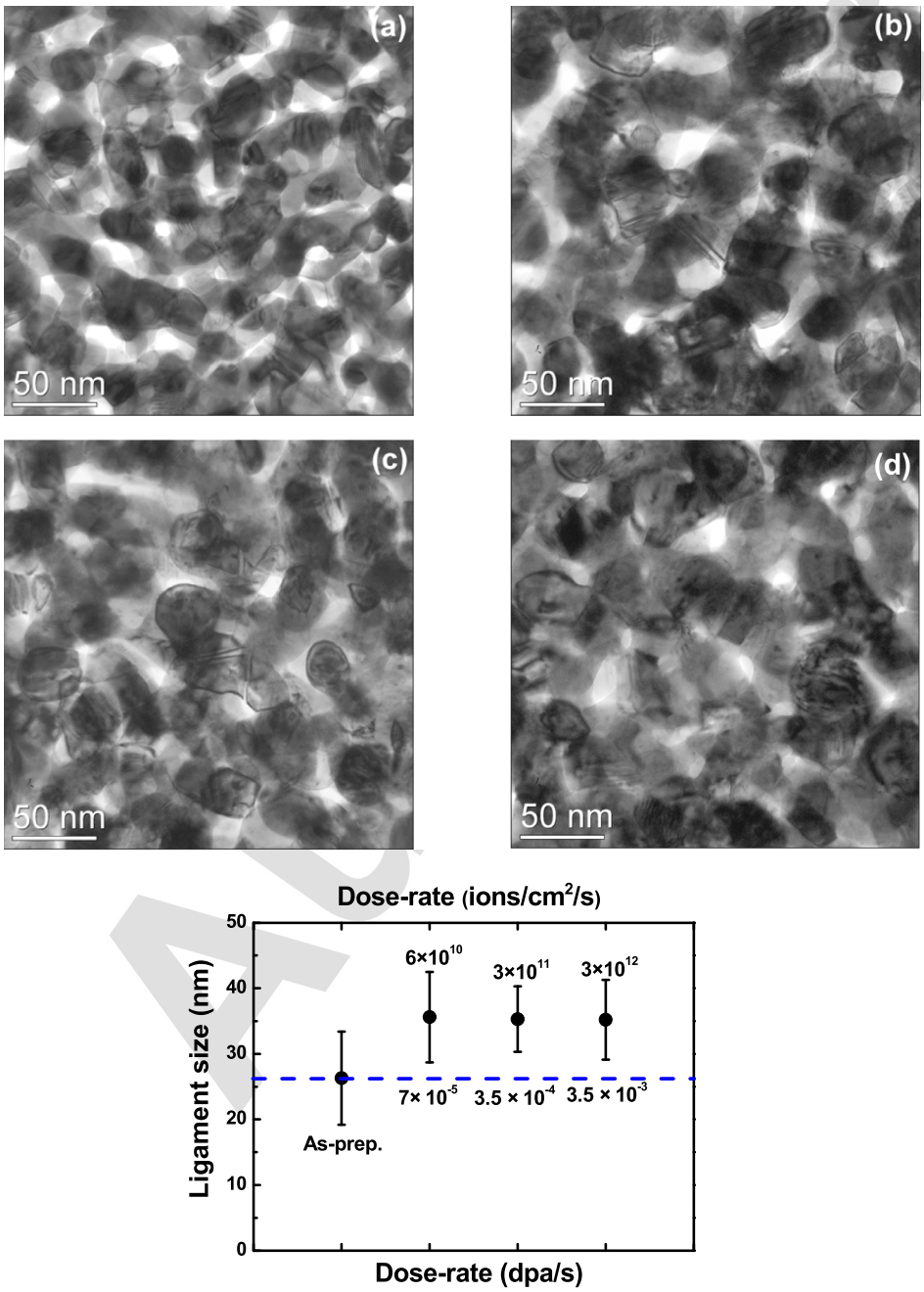

FIG. 1. TEM micrographs of (a) as-prepared np-Au and ion-irradiated np-Au foams irradiated at dose-rates of (b) 7×10^{-5} dpa/s, (c) 3.5×10^{-4} dpa/s, and (d) 3.5×10^{-3} dpa/s. (e) Ligament size as a function of ion dose rate and ion flux at room temperature irradiation.

irradiation, while retaining the foam structure. The figure suggests that radiation coarsening does not seem to depend on dose-rate. The comparison also shows that the ligament in the as-prepared np-Au foams (Fig. 1(a)) has fewer features than those observed in the ion-irradiated samples (Figs. 1(b)–1(d)).

Fig. 2 compares HRTEM images before and after irradiations. Pre-existing features such as twins, grain boundaries, and stacking faults are observed in the non-irradiated samples and remain after irradiation, where new features are also observed after ion irradiation. The straight lines in the samples are signatures of twin boundaries, which are very common in face-centered cubic (FCC) Au since the stacking fault energy of Au is low (32 erg/cm^2 (Ref. 25). Grain boundaries, which appear as curved lines in the micrographs, are observed in all specimens, indicating nanocrystalline structure of the np-Au foams. Dark dots are observed only in samples irradiated with high and intermediate dose-rates. HRTEM indicates they are stacking fault tetrahedra (SFT), the result of a collapse of vacancy clusters in low stacking fault energy materials.

Fig. 3(a) shows the magnified HRTEM image labeled by region 1 in Fig. 2(d). The defects with triangle shape are confirmed to be SFT by tilting the specimen under TEM. The corresponding fast Fourier transform (FFT) (Fig. 3(b)) shows that the SFT was observed along the Au zone axis [011].

To guide the analysis of these observations, we perform MD simulations of defect formation in Au ligaments during radiation damage. Our study is based on [001]-oriented cylindrical ligaments with 10 nm in diameter and 20 nm high, containing $\sim 1 \times 10^5$ atoms. The cylindrical geometries represent the individual ligaments forming the real nanoporous microstructure. Simulations were performed using the code LAMMPS[26] with an embedded atom model (EAM) potential for Au[27] together with a ZBL repulsive force at short distances. The ligament is equilibrated at 300 K until the surface

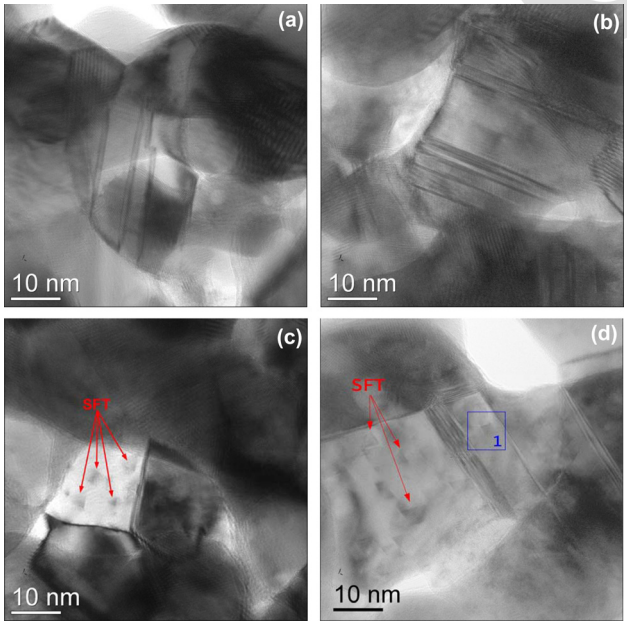

FIG. 2. High-resolution TEM images show the microstructures of (a) as-prepared np-Au foams and np-Au foam irradiated by 400 keV Ne^{++} ions at room temperature with dose-rates of (b) 7×10^{-5} dpa/s, (c) 3.5×10^{-4} dpa/s, and (d) 3.5×10^{-3} dpa/s. Grain boundaries and twins are observed in all samples. Stacking fault tetrahedra (SFTs) are observed in irradiated np-Au with dose-rate of 3.5×10^{-4} and 3.5×10^{-3} dpa/s.

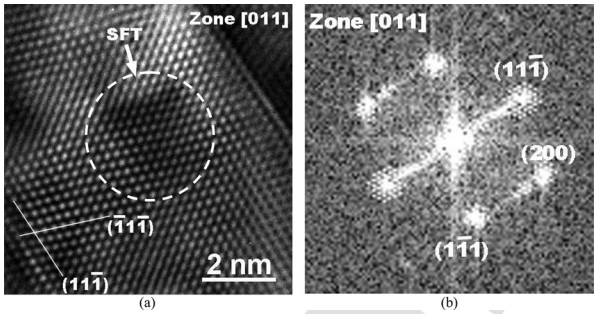

FIG. 3. (a) Atomic resolution image taken from Box 1 indicated in Fig. 2(d), shows ~2.2 nm large SFTs viewed along the [011] projection. (b) The corresponding FFT pattern with zone axis of [011].

induced stress is relaxed. Then, a primary knock-on atom (PKA) is created at the surface with 1.5 keV of kinetic energy with its velocity in the radial direction. We use an estimated low end of the PKA spectrum (i.e., 1.5 keV) expected from 400 keV Ne because our ligament diameter is smaller than the experimental. The resulting cascade is allowed to evolve for 20 ps after which the system is equilibrated back to 300 K. The 20 ps run is enough to propagate all damage throughout the ligament and produce a stable defect configuration within the MD simulation time. This procedure is repeated several times to investigate the effect of damage accumulation by multiple PKAs. Fig. 4 shows the response of the Au ligament after insertion of 1, 4, and 6 PKAs in (a)-(c), respectively. For clarity, Fig. 4(d) shows the SFT after removal of few vacancies that were surrounding it in Fig. 4(c). We observe that the ligament gets populated by individual vacancies and few self-interstitial atoms (SIA) at the end of each collision cascade. More SIA are formed during the initial stages of the collision cascade but as the ligament cools down they migrate to the surface or recombine with other vacancies, as happened to the SIA shown in Figs. 4(a) and 4(b) but not in Fig. 4(c).

As damage accumulates, vacancies agglomerate and form low-mobility clusters. Upon relaxation, the cluster collapses to form a SFT. Details of the formation mechanism can be found elsewhere.[28] Direct formation of SFTs due to a single collision cascade at higher energy has already been shown in bulk simulations,[29] but here the role of the surfaces as defect sinks, ligament size, and vacancy migration distance in the ligaments of np-Au foams is crucial to give SFT formation by accumulation of damage in multiple low energy cascades.

Our experimental and computational results indicate that np-Au foams respond to radiation damage in a substantially different way than bulk materials, providing a distinctive signature of the high surface/volume ratio effects. This signature is composed of three elements: coarsening, SFTs, and twins. Let us analyze them separately.

Coarsening: The fact that coarsening is dose-rate independent (see Fig. 1(e)) suggests that it is not due to an overall radiation-induced temperature rise, but rather, individual cascade effects. For 400 keV Ne ion irradiations, the spectrum of PKAs has a maximum energy of 133 keV, but exponentially more collisions happen at lower energies. From Fig. 3, in our previous work,[22] the highest-energy PKAs have enough energy to break ligaments smaller than ~5 nm, while those larger will likely survive the cascades with little damage. We

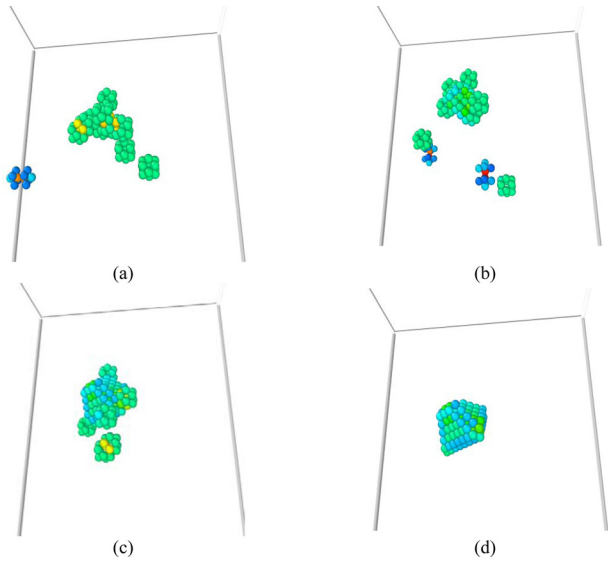

FIG. 4. Resultant configuration of a Au ligament with D:L 10:20 nm after insertion of 1.5 keV PKA. Only defective atoms are shown. (a) 1 PKA (b) 4 PKAs, and (c) 6 PKAs. All perfect FCC atoms are removed for clarity. (d) shows SFT in (c) after removal of few vacancies.

therefore conclude that melting of the smaller ligaments and little damage on the larger ligaments could be at the origin of the coarsening shown in Fig. 1(e). Another possible contribution to coarsening of np-Au foams could be radiation induced Au surface migration, an effect also enhanced by the local temperature rise expected after each cascade.

SFTs: Irradiation of thin film (bulk) gold to similar total doses shows interstitial and vacancy accumulation, in the form of dislocation loops and SFTs, respectively.[30,31] Our LAMMPS simulations for Au indicate the formation of SFTs in individual ligament due to the collapses of clusters. The fact is that we only observe SFTs in np-Au foams after they were irradiated at highest and intermediate dose-rate, whereas no SFTs were detected in the samples irradiated at lowest dose-rate. We believe that the combination of vacancy migration distance and ligament size in np-Au foams play a key role in determining the formation of SFTs at various dose-rates. An estimate of vacancy migration distance can be obtained by assuming that collision cascades occur within a representative volume element equal to L^3, where L is the ligament diameter. The time between cascades depends on the dose-rate and the size of representative volume. Our MD simulations for Au cascades in Au ligaments of size L suggest that each cascade produces ~10 vacancies; this number is in a reasonable agreement with an estimate using the modified Kinchin-Pease formula rescaled by an efficiency factor of 0.3, namely, the number of Frenkel pairs $N_d(E) = 0.3 \times 0.8E_v/(2E_d)$, where E_v is damage energy of 1.5 keV and E_d is displacement energy of 25 eV in current case. This number allows us to define the time between cascades as

$$t = 10/(dpa - rate \times number\ of\ atoms). \qquad (1)$$

The time between cascades for the three different dose-rate irradiations explored in this work, low (7.5×10^{-5} dpa/s), intermediate (3.5×10^{-4}), and high (3.5×10^{-3} dpa/s) dose-rates is equal to 0.095 s, 0.019 s, and 0.002 s for a ligament diameter $L \sim 25$ nm, i.e., number of atoms equal to $\sim 1.5 \times 10^6$ atoms.

Vacancy migration distance can be estimated from Einstein relation, $\langle r^2 \rangle = 6Dt$, where $\langle r^2 \rangle$ represents the mean-square distance traversed by the diffusing vacancies. Assuming the vacancy diffusion coefficient in pure gold at room temperature is $D = 5 \times 10^{-9}$ cm^2/s,[32] and a time between cascades calculated in Eq. (1) leads to vacancy migration distances equal to ~76 nm, 34 nm, and 11 nm for low, intermediate, and high dose-rate irradiations.

Formation of defects (SFTs) will depend on irradiation conditions defined by average cascade size and time between cascades. The simple approximations discussed above show that for the ligament size and dose-rates investigated in this work, vacancies generated in the low dose-rate irradiation regime will have the time to leave the ligament, while those generated at high dose-rate will not be able to diffuse before another cascade hits the representative volume. Therefore, at high dose rate vacancies accumulate and cluster, leading to the SFTs, as indicated by our simulation.

Another observation is that we did not observe dislocation loops in irradiated np-Au foams. No dislocation loops is a signature of interstitial annihilation at the surface of the foam, feature clearly confirmed by our computer simulations. Stage III in Au occurs at room temperature and therefore both interstitials and vacancies are mobile under our irradiation conditions. The higher mobility of interstitials gives them enough time between cascades at these dose-rates to annihilate, as demonstrated in the computer simulations.

Twins: In nanoscale ligaments, it is well known that dislocations do not have enough space to be stable, and that under plastic deformation partial dislocations are created at surfaces, travel all the way across the ligament, and disappear at opposite surfaces, leaving behind a staking fault in FCC crystals.[33] From geometric constraints, it is known that for macroscopic foams most of the plastic deformation occurs near the nodes between ligaments;[34,35] in our nanoscale case, we therefore expect to see a large number of twins or stacking faults close to the nodes, as in fact is shown in Figs. 1 and 2. Another mechanism for twin or stacking fault formation is apparent in computer simulations based on the stress induced by collision cascades. In fact, MD shows that a cascade close to a surface of a ligament easily creates SFTs running in all possible (111) planes and intersecting themselves in what comes out to be a stable defect.[36]

In summary, our work reports on the salient features of radiation damage in np-Au foams due to surface effect. We found that SFTs were formed when np-Au foams were irradiated at high dose-rate, but they were not created in np-Au foams at low dose-rate irradiation. Our combined experiments and simulation results indicate that the low dose-rate offers enough time interval for SIAs and vacancies to diffuse to the surface or recombine, whereas at the higher dose-rates explored, the time between cascades is shorter than the time needed for defect migration to the ligament surface, allowing vacancies to agglomerate and form SFTs. These findings suggest that nano-foams may display radiation tolerance in a particular region of the parameter space, namely, ligament size; they also identify some key factors governing radiation

damage development in nanoscale materials under irradiation, and therefore have important significance in understanding fundamental mechanisms of defect formation and in searching for radiation tolerant materials.

This work was funded by the Los Alamos's Laboratory Directed Research and Development (LDRD) Program. A.C. also acknowledges support from the DOE's Energy Frontier Research Center (EFRC) for Materials under Irradiation and Mechanical Extremes. E.M.B thanks funding from PICT2009-0092. The Center for Integrated Nanotechnologies (CINT) is acknowledged for facilitating the synthesis capabilities and J. Tesmer and the IBML team are acknowledged for their help in performing ion irradiations.

[1]S. J. Zinkle and N. M. Ghoniem, J. Nucl. Mater. **417**, 2 (2011).
[2]J. F. Rodriguez-Nieva, E. M. Bringa, T. A. Cassidy, R. E. Johnson, A. Caro, M. Fama, M. J. Loeffler, R. A. Baragiola, and D. Farkas, Astrophys. J. Lett. **743**, L5 (2011).
[3]C. N. R. Rao and A. K. Cheetham, J. Mater. Chem. **11**, 2887 (2001).
[4]E. G. Fu, J. Carter, G. Swadener, A. Misra, L. Shao, H. Wang, and X. Zhang, J. Nucl. Mater. **385**, 629 (2009).
[5]A. Misra, X. Zhang, M. J. Demkowicz, R. G. Hoagland, and M. Nastasi, Mater. Res. Soc. Symp. Proc. **1188**, LL06-01 (2009).
[6]E. G. Fu, A. Misra, H. Wang, L. Shao, and X. Zhang, J. Nucl. Mater. **407**, 178 (2010).
[7]G. R. Odette and D. T. Hoelzer, JOM **62**, 84 (2010).
[8]A. Kimura, R. Kasada, N. Iwata, H. Kishimoto, C. H. Zhang, J. Isselin, P. Dou, J. H. Lee, N. Muthukumar, T. Okuda, M. Inoue, S. Ukai, S. Ohnuki, T. Fujisawa, and T. F. Abe, J. Nucl. Mater. **417**, 176 (2011).
[9]E. A. Marquis, Appl. Phys. Lett. **93**, 181904 (2008).
[10]A. Misra, M. J. Demkowicz, X. Zhang, and R. G. Hoagland, JOM **59**, 62 (2007).
[11]J. Biener, A. M. Hodge, and A. V. Hamza, Appl. Phys. Lett. **87**, 121908 (2005).
[12]Y. Sun, J. Ye, A. M. Minor, and T. J. Balk, Microsc. Res. Tech. **72**, 232 (2009).
[13]Y. Sun, J. Ye, Z. Shan, A. M. Minor, and T. J. Balk, JOM **59**, 54 (2007).
[14]L. A. Zepeda-Ruiz, B. Sadigh, J. Biener, A. M. Hodge, and A. V. Hamza, Appl. Phys. Lett. **91**, 101907 (2007).
[15]P. Erhart, E. M. Bringa, M. Kumar, and K. Albe, Phys. Rev. B **72**, 052104 (2005).
[16]J. Biener, A. M. Hodge, J. R. Hayes, C. A. Volkert, L. A. Zepeda-Ruiz, A. V. Hamza, and F. F. Abraham, Nano. Lett. **6**, 2379 (2006).
[17]D. A. Crowson, D. Farkas, and S. G. Corcoran, Scr. Mater. **61**, 497 (2009).
[18]J. Erlebacher, M. J. Aziz, A. Karma, N. Dimitrov, and K. Sieradzki, Nature (London) **410**, 450 (2011). AQ2
[19]K. Kolluri and M. J. Demkowicz, Acta Mater. **59**, 7645 (2011).
[20]B. Hyde, H. D. Espinosa, and D. Farkas, JOM **57**, 62 (2005).
[21]J. Biener, A. Wittstock, L. A. Zepeda-Ruiz, M. M. Biener, V. Zielasek, D. Kramer, R. N. Viswanath, J. Weissmüller, M. Bäumer, and A. V. Hamza, Nature Mater. **8**, 47 (2009).
[22]E. M. Bringa, J. D. Monk, A. Caro, A. Misra, L. Zepeda-Ruiz, M. Duchaineau, F. Abraham, M. Nastasi, S. T. Picraux, Y. Q. Wang, and D. Farkas, Nano Lett. **12**, 3351 (2012).
[23]L. R. Doolittle, Nucl. Instrum. Methods Phys. Res. B **9**, 344 (1985).
[24]J. F. Ziegler, J. P. Biersack, and U. Littmark, *The Stopping and Ranges of Ions in Matter* (Pergamon, NY, USA, 1985).
[25]M. L. Jenkins, Philos. Mag. **26**, 747 (1972).
[26]S. J. Plimpton, J. Comput. Phys. **117**, 1 (1995).
[27]S. M. Foiles, M. I. Baskes, and M. S. Daw, Phys. Rev. B **33**, 7983 (1986).
[28]B. N. Singh, S. I. Golubov, H. Trinkaus, D. J. Edwards, and M. Eldrup, J. Nucl. Mater. **328**, 77 (2004).
[29]K. Nordlund and F. Gao, Appl. Phys. Lett. **74**, 2720 (1999).
[30]S. Ishino, N. Sekimura, K. Hirooka, and T. Muroga, J. Nucl. Mater. **141–143**, 776 (1986).
[31]N. Ajika, H. Hashimoto, and Y. Takai, Phys. Status Solidi A **87**, 235 (1985).
[32]G. De Lorenzi and F. Ercolessi, Europhys. Lett. **20**, 349 (1992).
[33]C. R. Weinberger and W. Cai, J. Mater. Chem. **22**, 3277 (2012).
[34]M. F. Ashby, Metall. Mater. Trans. A **14**(9), 1755 (1983). AQ3
[35]A. G. Evans, J. W. Hutchinson, and M. F. Ashby, Prog. Mater. Sci. **43**, 171 (1999). AQ4
[36]L. A. Zepeda-Ruiz, "■" (unpublished). AQ1